Morphological analysis of Gissane's angle utilising a statistical shape model of the calcaneus

Morphological Analysis of Gissane's Angle Utilising a Statistical Shape Model of the Calcaneus

Beat Schmutz*, Marcel Lüthi, Yohan Kai Schmutz-Leong, Ryan Shulman, Simon Platt

1. Dr Beat Schmutz, PhD
Institute of Health and Biomedical Innovation
Queensland University of Technology
60 Musk Avenue, Kelvin Grove QLD 4059, Australia

Jamieson Trauma Institute
Metro North Hospital and Health Service
Herston QLD 4029, Australia

Email: b.schmutz@qut.edu.au

*Corresponding author

2. Dr Marcel Lüthi, PhD
Department of Mathematics and Computer Science
University of Basel
Spiegelstrasse 1, 4051 Basel, Switzerland

Email: marcel.luethi@unibas.ch

3. Mr Yohan Kai Schmutz-Leong, BBiomedSc
Institute of Health and Biomedical Innovation
Queensland University of Technology
60 Musk Avenue, Kelvin Grove QLD 4059, Australia

Email: yohan.kai39@gmail.com

4. Dr Ryan Shulman, MD, FRANZCR
Queensland X-Ray
Mater Hospital Brisbane
301 Vulture St, South Brisbane QLD 4101, Australia

Email: ryans79@hotmail.com

5. Dr Simon Platt, MD, FRCS, FRACS
Department of Orthopaedic Surgery
Gold Coast University Hospital
1 Hospital Boulevard, Southport QLD 4215, Australia

Email: simonplatt@me.com

ABSTRACT

Introduction

Gissane's crucial angle (GA) facilitates to diagnose calcaneal fractures, and serves as an indicator of the quality of anatomical reduction after fixation. The study aimed to utilise statistical shape models (SSM) for analysing the complex 3D surface anatomy of the calcaneus represented by the simplified GA measurement on lateral radiographs.

Materials and Methods

SSMs were generated from CT scans of paired adult calcanei from 10 Japanese and 31 Thai specimens. GA measurements in 3D and 2D were obtained for the lateral, central and medial anatomy of the posterior facet and sinus tarsi. The correlation between calcaneal length and GA was analysed. Regression and principal component (PC) analyses were conducted for analysing morphological variability in calcaneal shape relating to GA. The bilateral symmetry of the obtained measurements was analysed.

Results

The mean GA (lateral) for the Japanese specimens was 105.1° ± 7.5 and 105.4° ± 8.5 for the Thai. The projected 2D angles of the central and medial measurements were larger ($P < 0.00$) than the 3D values. The medial projected 2D angles were larger ($P \leq 0.02$) compared to the lateral. Despite the bilateral symmetry of GA and calcaneal length, their correlation displayed clear signs of asymmetry, which was confirmed by regression and PC analyses.

Conclusions

Japanese and Thai specimens revealed lower GAs (both range and mean) compared to reported reference values of other ethnicities. As a reduced GA is generally indicative of a calcaneal fracture, our results are important to surgeons for their diagnostic assessment of Japanese and Thai patients. The results indicate that the GA measurement on a plain radiograph is a simplified representation of the lateral to central 3D calcaneal anatomy but significantly underestimates the angle measurement on the medial aspects of the respective surface areas.

Keywords: Gissane's angle, calcaneus, statistical shape model, morphology

INTRODUCTION

The calcaneus is the largest tarsal bone; its morphology is both unique and complex, playing a critical role in weight bearing. Owing to its complexity and multiple articulations linking the ankle and hindfoot, disruption of calcaneal anatomy can alter the biomechanics of the foot and lower limb. Calcaneal fractures account for up to 75% of all foot fractures and 1-2% of all fractures; they are complex, life-altering injuries that are difficult to treat and manage [1; 19; 20]. Besides Boehler's angle, Gissane's crucial angle (GA) facilitates both to diagnose calcaneal fractures, and to assess the quality of anatomical reduction after fixation. Generally, a reduced GA on a lateral radiograph is indicative of a fracture [10; 20]. Within the relevant literature, normal GAs have been reported in the range of 96° to 152°. Such a wide range of mean GA values is reflective of the difference in calcaneal anatomy between ethnicities [9; 24]. To our knowledge, no reference values of Gissane's angle for Japanese and Thai subjects have yet been reported in English literature.

Clinically, Gissane's angle is defined on a lateral radiograph by two strong cortical struts, one extending along the lateral border of the posterior facet to the fossa calcanei and the other from the fossa along the lateral border of the sinus tarsi [10]. Thus, GA measured on a 2D x-ray represents the lateral 3D anatomy of the posterior facet and sinus tarsi. As such, GA represents radiographic superimposition of two irregular and non-planar 3D surfaces, the convex surface of the posterior facet and the concave surface of the sinus tarsi. However, to our knowledge, the anatomy of these two surfaces medial to the lateral edge has not yet been quantified in relation to GA. When Gissane defined the parameter [6] plain radiology was the primary imaging modality. There is no doubt that the angle is a very helpful tool to asses for fracture and estimate an adequacy of reduction, it must be borne in mind that GA reduces a complex anatomic area into a 2D projection on a plain radiograph.

In recent years, the use of statistical shape models (SSMs) to analyse the anatomical variability of bones has gained traction and attention [3; 5; 12; 14; 22; 28-30]. Melinska et al. 2015 were the first to generate a SSM of the calcaneus [14]. While measurements of GA on a 3D model were recorded, the correlation of the 3D measurement to the corresponding 2D measurement on a lateral projection plane was not reported or analysed. More recently, Tümer et al. 2018 described the use of a SSM's principal components (PCs) for evaluating bone shape variations in the principal directions, to express the most variance in the shape of calcaneal samples [28]. Whilst it was mentioned that PC7 would impact Gissane's angle, no measurements of the angle were obtained; hence, the impact was not quantified.

Therefore, the five aims of our study were to first establish whether GA measurements of Japanese and Thai calcanei are within the reported ranges of reference values of other ethnicities. Second, to determine whether the GA measurement on a lateral radiograph is representative for the 3D surface anatomy medial to the lateral aspect of posterior facet and sinus tarsi. Third, to formally determine which PC(s) is/are significantly associated with GA measurements. Fourth, to find out whether maximum calcaneal length correlates with GA measurements. Finally, to determine whether any of the obtained measurements display bilateral asymmetric trends.

MATERIALS AND METHODS

3D bone models

Post-mortem CT scan data of 41 paired Japanese and Thai Calcanei was obtained from the Virtual Bone Morphology Database at the Institute of Health and Biomedical Innovation. Of the 41 specimens, 10 were Japanese (5 male, mean age 66.2 years, range 53-78) and 31 were Thai (17 males, mean age 67.4 years, range 44-90). Upon visual inspection, all specimens exhibited calcaneal morphology within the normal range. The 3D bone models were reconstructed from CT images by utilising the Watershed Segmentation Tool of the image processing and 3D reconstruction software Avizo 2019.1 (Visualization Sciences Group, Merignac, France). Manual segmentation was performed where the Watershed Tool failed to correctly demarcate the bony surface.

Statistical Shape Model

The framework for generating the statistical bone model is based on Gaussian Process Morphable Models (GPMMs), which are a generalised form of point distribution models (PDMs). The processing and mathematical background of GPMMs, has previously been described in detail by Lüthi et al. [12; 13], and as such, the following summarises only the main steps. First, all calcanei models were rigidly aligned to a randomly selected reference calcaneus. The surface of the reference was subsequently warped to fit each of the calcanei models. Such non-rigid registration brings all the shapes into correspondence, whereby for each point on the reference, the corresponding point on each calcaneal model is identified. This allows for a pointwise computation of the mean and variance for the SSM by way of Principal Component Analysis (PCA). The mean shape of the model is a fully 3D morphological mean bone.

To reduce potential bias introduced by choosing a specific reference bone, two SSMs were built for the right calcaneus, where the mean SSM of the first iteration was used as reference in the second iteration for generating the final statistical mean 3D model. All left calcaneal bone models were mirrored to the right side and registered to the right mean SSM generated in the first iteration. Hence, the same reference bone was used to generate the SSM of both the left and right calcaneus. The mean shape of the statistical calcaneus 3D bone model was generated via the open source shape modelling software library, Scalismo [7].

3D Measurements of Gissane's Angle

On digital lateral radiographs, Gissane's angle is typically measured with a screen protractor superimposed over the relevant anatomical structure. Currently, only two studies [8; 14], have reported measurements of GA on 3D bone models where three landmark points were used for the angle calculation. However, our observations would suggest that, in certain instances, the use of only three landmark points is insufficient. For bones with a pronounced calcaneal fossa, setting the landmark of the angle apex at this location resulted in an underestimation of the anatomical angle measurement. Therefore, in our study we have used four landmark points as this enables for the generation of vectors representing the lateral margins of the posterior facet and sinus tarsi, respectively (see Fig. 1).

In addition to the standard measurement at the lateral aspect, GA was also measured at the medial aspect as well as in the centre of the posterior facet and the sinus tarsi (Figure 1). Gissane's angles measured at the lateral, medial and centre aspects of the bone model were termed GAL-3D, GAM-3D and GAC-3D, respectively.

Two experienced clinicians (orthopaedic surgeon, radiologist) generated five sets of eight landmarks each for measuring GA and for analysing the intra- and inter-observer reliability in the angle calculations. The landmarks defined on the right mean SSM were also used for measuring GA on all left calcanei. The three GAs were measured for all calcanei as well as for the Japanese and Thai subgroups. The angle calculations from the corresponding landmark pairs were coded in Scalismo and the 3D GA measurements were obtained by batch processing all bone models.

2D Measurements of Gissane's Angle

In order to compare our 3D GA measurements to clinical lateral x-ray measurements, we have projected all 3D landmarks onto a lateral projection plane where they were used for calculating the corresponding 2D GAs. An experienced orthopaedic surgeon defined the lateral projection plane by aligning the right mean SSM such that its position, based on visual assessment, is equivalent to a calcaneus on a lateral x-ray (see Figure 1). The same projection plane was used for measuring GA on the left calcanei. The landmark 3D to 2D projections and the angle calculations on the projection plane were coded in Scalismo and the 2D GA measurements were obtained by batch processing all bone models.

Measurement of Calcaneus Maximum Length

The maximum length of the calcaneus was defined as the linear distance between the most anterior point of the calcaneus and the posterior most point on the calcaneal tuberosity [15]. Calcaneal length was measured as the distance between two planes orthogonal to the long bone axis and fitted at the most anterior and posterior points on a bone model (see Figure 1). Bone length was measured using tools of the reverse engineering software Rapidform2006 (Inus Technology, Seoul, Korea) as this was more efficient compared to coding the measurement in Scalismo.

Regression Analysis of PCs and GAL-3D

The SSM was used to analyse which changes in the shape correlated to changes in the Gissane's angle (GAL-3D). For this, an ordinary linear regression was performed. The coefficients corresponding to the first 10 principal components as the independent variables and Gissane's angle as the dependent variable were used. In order to assess the sensitivity of the results with respect to different landmark placements and inter observer variations, we performed an independent regression analysis for each landmark set defined by each clinical expert.

Shape changes associated with these principal components are demonstrated by colour coding the distances, which result from changing the shape coefficients of an arbitrary shape, one unit in the direction defined by the correlation coefficients. The intuition behind this visualisation is, that the components that show a strong (negative or positive) correlation, will lead to a large shape change, whereas a change in a coefficient with a correlation close to zero will not change the result. For details, we refer to [4].

Statistical Data Analysis

The level of statistical significance was set to $p < 0.05$ for all tests, which were conducted with standard statistical software (IBM SPSS Statistics 24.0; Chicago, IL, USA). In a first step, descriptive statistics for GA and bone length were produced. As some of the angle measurements were non-uniformly distributed, we have performed non-parametric statistical analyses. In a second step, to test for significant side and ethnicity differences in the GA and bone length measurements as well as between GA measurements, the Wilcoxon Signed Ranks test was used for paired samples and the Mann-Whitney U test for independent samples. In a third step, associations between bone length and GA, and between 3D GA and 2D GA measurements were explored using correlation analyses after Spearman. In the final step, we determined the intra- and inter-observer reliability for GA by calculating the intra-class correlation coefficients. The intra-class reliability was calculated using a 2-way mixed-effects, absolute agreement, and single measurement model. Whereas for the inter-class reliability a 2-way random-effects, absolute agreement, and single measurement model was used [11; 27]. The guidelines by Koo and Li [11] were used for the interpretation of the ICC.

RESULTS

Mean SSM of Asian calcanei

The mean left and right SSMs generated from 41 Asian specimens are shown in Figure 2. Upon visual inspection, the left and right calcaneus show similar general patterns of morphological variability. Notably, variances of the left appear to be slightly larger at the lateral process of the calcaneal tuberosity.

Gissane angle measurements

The mean Japanese and Thai Gissane angles of the five repeated measurements by two raters are summarised in Tables 1 and 2. There were no statistically significant differences between the corresponding angles of the two ethnicities. Apart from GAM-2D for the Japanese samples, there was bilateral symmetry for all other GA measurements.

The mean differences and correlations between the 3D and 2D Gissane angles of the five repeated measurements by two raters are summarised in Table 3. For the projected 2D angles the differences between GAL and GAM were significant for both the left ($P = 0.020$) and right ($P = 0.005$) side. Whereas the difference between GAL and GAC were neither significant for the left ($P = 0.112$) nor the right ($P = 0.077$) side.

Correlation of Gissane's angle with maximal bone length

The mean maximal length of the calcaneus from the 41 Asian subjects is summarised in Table 4. There was no statistically significant difference between left and right measurements nor between the two ethnicities.

The correlations between Gissane's angle and calcaneus maximum length are summarised in Table 5.

Reliability analysis

The intraclass correlations of five repeated GA measurements by the two raters ranged from 0.210 (lower: 0.031, upper: 0.448, p = 0.000) for GAM-3D to 0.741 (lower: 0.536, upper: 0.860, p = 0.000) for GAL-3D. The results of the inter observer reliability for the GA measurements are summarised in Table 6. The interclass correlations were calculated from the respective mean of five repeated GA measurements by each rater.

Regression Analysis of PCs and GAL-3D

The regression analysis of the first 10 principal components using the pooled data of the five repeated measurements from both raters reveals a clear bilateral asymmetry in the PCs associations with Gissane's angle (Table 7). While on the left, PC7 showed the strongest correlation with GAL-3D on the right it was the weakest of the four PCs with significant associations. More striking, PC1 displayed the strongest correlation on the right side followed by PC10 and PC8, while on the left none of them was significantly associated with Gissane's angle.

The bilateral asymmetry in the calcaneal anatomy associated with Gissane's angle is also evident from Figure 3, which shows a clear difference between the correlations of the left and right bone length, sinus tarsi and the GAL-3D measurements.

DISCUSSION

Our results reveal that for Gissane's angle measured at the lateral aspect of the calcaneus, the 2D measurements very strongly and significantly correlate with the 3D measurements (Table 3). Although the difference between 3D and 2D measurements was statistically significant for the left side and marginally non-significant for the right, the very small mean differences of < 0.25° is clinically insignificant. As our 2D projection plane was defined by an experienced clinician, the obtained results indicate that measuring GA on the lateral aspect of a 3D model would also closely represent the measurement on a lateral radiograph. Hence, the GAL-2D measurements of this study of 105.1° and 105.4° can be used as first reference values of Gissane's angle in Japanese and Thai patients, respectively. Our Japanese and Thai mean and minimum GA measurements are lower than any of the values reported for other ethnicities (Table 8) [9; 24-26]. As a lower GA is generally indicative of a calcaneal fracture, this information is of vital importance and significance to the surgical community for the diagnostic assessment of Japanese and Thai patients.

While the medial and centre 2D GA measurements highly and significantly correlated with the 3D values (Table 3), the 2D GA measurements are both statistically and clinically significantly larger (GAM: ~20°, GAC: >6°). This discrepancy is caused by the third dimension (mediolateral) resulting in projection differences between 3D and 2D GA measurement, as evident from Figure 1. Therefore, prior to comparative analyses, GA measurements on a 3D model, medial to the lateral aspect of the posterior facet and sinus tarsi, need to be projected onto a plane representing the lateral radiographic imaging plane. Our results reveal that the projected 2D GA measured on the medial side is significantly larger compared to GA on the lateral side, particularly for the Japanese specimens (Tables 1 & 2). In contrast, the projected central and lateral 2D GA measurements were comparable.

The maximum calcaneal length of 75.8 mm of our Japanese sample (Table 4) was larger compared to the 70.9 mm (male and female average) reported by Sakaue et al. [21]. This difference is likely due to Sakaue et al. having included subjects as young as 14 years in their study. For our Thai samples, the maximum length of 76.6 mm closely matches the 76.9 mm (male and female average) published by Scott et al. [23]. The bilateral symmetry for the maximum length of the calcaneus for both of our samples is in agreement with findings from studies of other ethnicities [15; 16].

There was no statistically significant correlation between calcaneus length and any of the measured Gissane angles, despite moderately strong correlations for several angles (Table 5). Striking is the significant difference in correlation coefficients between body sides. While all left GAs in the Japanese and both left medial GAs in the Thai show a negative correlation, all right GAs display a positive one. This apparent asymmetry in length to GA correlations appears to contradict the observed symmetry in the length and GA (except GAM-2D in Japanese) measurements. However, the regression analysis of the PCs association with GAL-3D also displays a distinct asymmetrical trend (Table 7). On the right side, PC1, which is associated with changes in bone length [28], significantly correlates with Gissane's angle, but not on the left. This observation is further confirmed by Figure 3, which clearly shows that only for the right side there is a correlation between bone length and GA. Our study formally confirms Tümer et al.'s [28] reported association of PC7 with the anatomy represented by GA. However, our results clearly reveal that besides PC7 there are other PCs which significantly correlate with Gissane's angle. Our reported existence of local asymmetries in the calcaneus is corroborated by other anatomical studies [15; 18]. This bilateral asymmetry can be explained by differences in biomechanical loading of the dominant versus the non-dominant lower limb, which have been shown to impact on bone morphology [2]. To the clinician, particularly those reconstructing calcaneal fractures, the fact that isolated calcanei should be considered individual entities must be remembered when restoring shape.

While the intraclass correlations of our two raters for the GA measurements ranged from poor to high moderate, the combined mean ICC of 0.72 for GAL-3D and 0.70 for GAL-2D are considerably higher than the reported values of 0.39 and 0.52 [10; 17]. In the reported clinical studies, raters measured GA on the x-ray of each subject. However, in our study, the landmarks defined on the right mean 3D SSM were used for the GA measurements on all individual bone models. This was made possible through the SSM framework which established correspondence between bone models. Therefore, it is reasonable to expect that our approach will translate into a higher intra-rater agreement.

The high consensus of our two raters is reflected by the good to excellent interclass correlations of 0.86 – 0.97 for GAL and GAC for both 3D and 2D measurements (Table 6). While the ICC for the 3D GAM was in the medium moderate range, there was good to excellent agreement for the projected 2D measurement. This difference between 3D and 2D measurements is likely due to differences in landmark positions in the mediolateral direction affecting the inclination of GA on the 3D model compared to the 2D GA measured from the projected landmarks. Our high inter-rater agreements are in stark contrast to the reported ICC of 0.28 [17]. It must be noted, that part of this large discrepancy is the result of calculating the ICC in our study from the mean of five repeated

measurements by each of the raters. A further potential cause for difference is that in our study the landmarks for the GA measurement were defined on a 3D bone model whereas in the clinical study this was done on 2D radiographs. At present, it is unknown to what extent the method of landmark selection affects the reliability of the GA measurement.

The main limitation of our study is the relatively small sample size, particularly for the Japanese specimens, which might impact the validity and applicability of the reported results. A further limitation is that we did not compare our 3D GA measurements directly to corresponding measurements on standard clinical lateral radiographs, but to measurements on a defined lateral projection plane. However, as our lateral projection plane was defined by an experience clinician and since our 3D lateral GA measurements were in very close agreement and strongly correlated with the corresponding 2D measurements, it would be reasonable to expect similar results from a direct comparison with clinical x-rays.

CONCLUSIONS

Our results indicate that the mean and range of GA for Japanese and Thai calcanei is below the reported reference values from other ethnicities. This is of clinical importance as a lower GA is generally indicative of a calcaneal fracture. The GA on the medial aspect of the posterior facet and sinus tarsi is significantly larger than on the lateral side, which highlights that this area of sophisticated geometry is oversimplified by the standard 2D radiological parameters. This is corroborated by the finding that multiple PCs are associated with the anatomy represented by GA, and the observed bilateral asymmetry between them. Our findings demonstrate that a good to excellent interclass agreement can be achieved by utilising the mean of repeated GA measurements, which we recommend for reporting GA measurements in future studies.

COMPLIANCE WITH ETHICAL STANDARDS

Ethical approval

The CT data utilised was available from studies previously published.

ACKNOWLEGDMENT

The study was supported in part through a Scientific Exchanges Grant (IZSEZO_186525) from the Swiss National Science Foundation.

REFERENCES

1 Adams M, Munz J, Koury K (2017) Fractures of the Calcaneus. Instr Course Lect., 66:51-61

2 Auerbach BM, Ruff CB (2006) Limb bone bilateral asymmetry: variability and commonality among modern humans. Journal of Human Evolution, 50(2):203-218

3 Bah MT, Shi J, Browne M, et al. (2015) Exploring inter-subject anatomic variability using a population of patient-specific femurs and a statistical shape and intensity model. Medical Engineering and Physics, 37(10):995-1007

4 Blanz V, Vetter T (1999) A morphable model for the synthesis of 3D faces. Proceedings of the 26th annual conference on Computer graphics and interactive techniques. ACM Press/Addison-Wesley Publishing Co., pp 187-194

5 Daruwalla ZJ, Courtis P, Fitzpatrick C, Fitzpatrick D, Mullett H (2010) An application of principal component analysis to the clavicle and clavicle fixation devices. Journal of Orthopaedic Surgery and Research, 5:21-21

6 Gissane W (1947) Discussion on fractures of the os calcis. Annual Meeting of the British Orthopaedic Association, London, 1946. J Bone Joint Surg (Br)(29):255

7 Gravis Group (2016) Scalismo - scalable image analysis and shape modelling. University of Basel. https://scalismo.org/. Accessed 22 February 2020

8 Idram I, Lai J-Y, Lee P-Y (2019) A reliable method for morphological measurement of 3D calcaneus models from computed tomography images. Biomedical Research, 30(1):149-159

9 Khoshhal K, Ibrahim A, Al-Nakshabandi N, Zamzam M, Al-Boukai A, Zamzami M (2004) Böhler's and Gissane's angles of the calcaneus in the Saudi population. Saudi Med J 25:1967-1970

10 Knight JR, Gross EA, Bradley GH, Bay C, LoVecchio F (2006) Boehler's angle and the critical angle of Gissane are of limited use in diagnosing calcaneus fractures in the ED. The American Journal of Emergency Medicine, 24(4):423-427

11 Koo TK, Li MY (2016) A Guideline of Selecting and Reporting Intraclass Correlation Coefficients for Reliability Research. J Chiropr Med, 15(2):155-163

12 Lüthi M, Albrecht T, Gass T, et al. (2012) Statismo - a framework for pca based statistical models. The Insight Journal, 1:1-18

13 Lüthi M, Gerig T, Jud C, Vetter T (2018) Gaussian Process Morphable Models. IEEE Transactions on Pattern Analysis and Machine Intelligence, 40(8):1860-1873

14 Melinska A, Romaszkiewicz P, Wagel J, Sasiadek M, Iskander D (2015) Statistical, Morphometric, Anatomical Shape Model (Atlas) of Calcaneus. PLoS ONE 10(8):e0134603

15 Nathena D, Michopoulou E, Kranioti EF (2017) Sexual dimorphism of the calcaneus in contemporary Cretans. Forensic Science International, 277:260.e261-260.e268

16 OTAĞ İ, TETİKER H, TAŞTEMUR Y, SABANCIOĞULLARI V, KOŞAR M, ÇİMEN M (2017) Morphometric Measurements of Calcaneus; Boehler'sangle and bone length estimation. Cumhuriyet Üniversitesi Fen Edebiyat Fakültesi Fen Bilimleri Dergisi, 38 (2):256-263

17 Otero JE, Westerlind BO, Tantavisut S, et al. (2015) There is poor reliability of Böhler's angle and the crucial angle of Gissane in assessing displaced intra-articular calcaneal fractures. Foot and Ankle Surgery, 21(4):277-281

18 Prasad SA, Rajasekhar SSSN (2019) Morphometric analysis of talus and calcaneus. Surgical and Radiologic Anatomy, 41(1):9-24

19 Rammelt S, Sangeorzan BJ, Swords MP (2018) Calcaneal Fractures - Should We or Should We not Operate? Indian journal of orthopaedics, 52(3):220-230

20 Razik A, Harris M, Trompeter A (2018) Calcaneal fractures: Where are we now? Strategies in trauma and limb reconstruction (Online), 13(1):1-11

21 Sakaue K (2011) Sex Assessment from the Talus and Calcaneus of Japanese. Bull. Natl. Mus. Nat. Sci., 37:35-48

22 Sarkalkan N, Weinans H, Zadpoor AA (2014) Statistical shape and appearance models of bones. Bone, 60:129-140

23 Scott S, Ruengdit S, Peckmann TR, Mahakkanukrauh P (2017) Sex estimation from measurements of the calcaneus: Applications for personal identification in Thailand. Forensic Science International, 278:405.e401-405.e408

24 Sengodan V, Amruth K, K (2012) Bohler's and Gissane Angles in the Indian Population. Journal of Clinical Imaging Science, 2(1):77-77

25 Seyahi A, Uludağ S, Koyuncu L, Atalar A, Demirhan M (2009) The calcaneal angles in the Turkish population. Acta Orthop Traumatol Turc, 43:406-411

26 Shoukry FA, Aref YK, Sabry AAE (2012) Evaluation of the normal calcaneal angles in Egyptian population. Alexandria Journal of Medicine, 48(2):91-97

27 Shrout PE, Fleiss JL (1979) Intraclass correlations: Uses in assessing rater reliability. Psychological Bulletin, 86(2):420-428

28 Tümer N, Arbabi V, Gielis WP, et al. (2019) Three-dimensional analysis of shape variations and symmetry of the fibula, tibia, calcaneus and talus. Journal of Anatomy, 234(1):132-144

29 van IJsseldijk EA, Valstar ER, Stoel BC, et al. (2016) Three dimensional measurement of minimum joint space width in the knee from stereo radiographs using statistical shape models. Bone and Joint Research, 5(8):320-327

30 Zhang J, Hislop-Jambrich J, Besier TF (2016) Predictive statistical models of baseline variations in 3-D femoral cortex morphology. Medical Engineering & Physics, 38(5):450-457

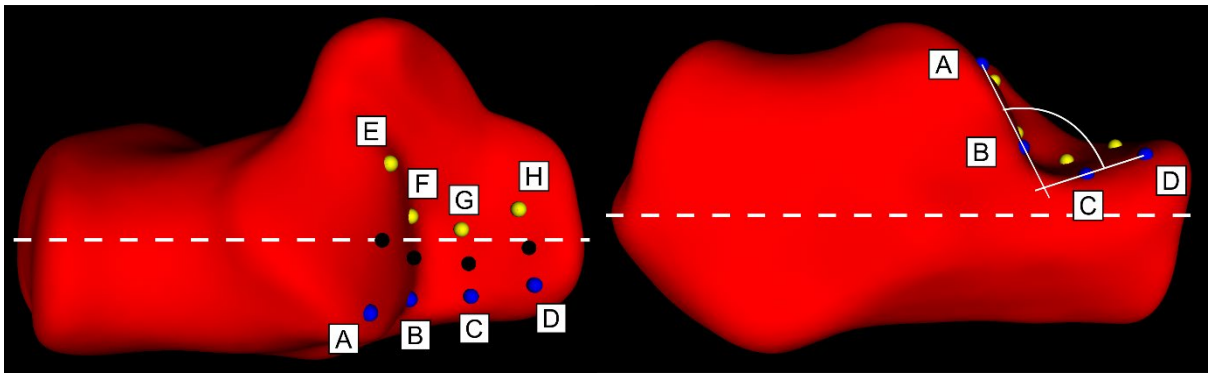

Figure 1. Landmarks selected on the right mean calcaneus model for calculating Gissane's angle. Four landmarks each were selected on the lateral (blue dots) and medial (yellow dots) aspects of the posterior facet and sinus tarsi, respectively. The mid points (black dots) between corresponding landmark pairs were calculated and used for measuring the centre Gissane angle. The dotted white line indicates the position of the vector used for measuring bone length. The projection plane for the 2D GA measurements was defined by the dotted line and parallel to the image plane on the right.

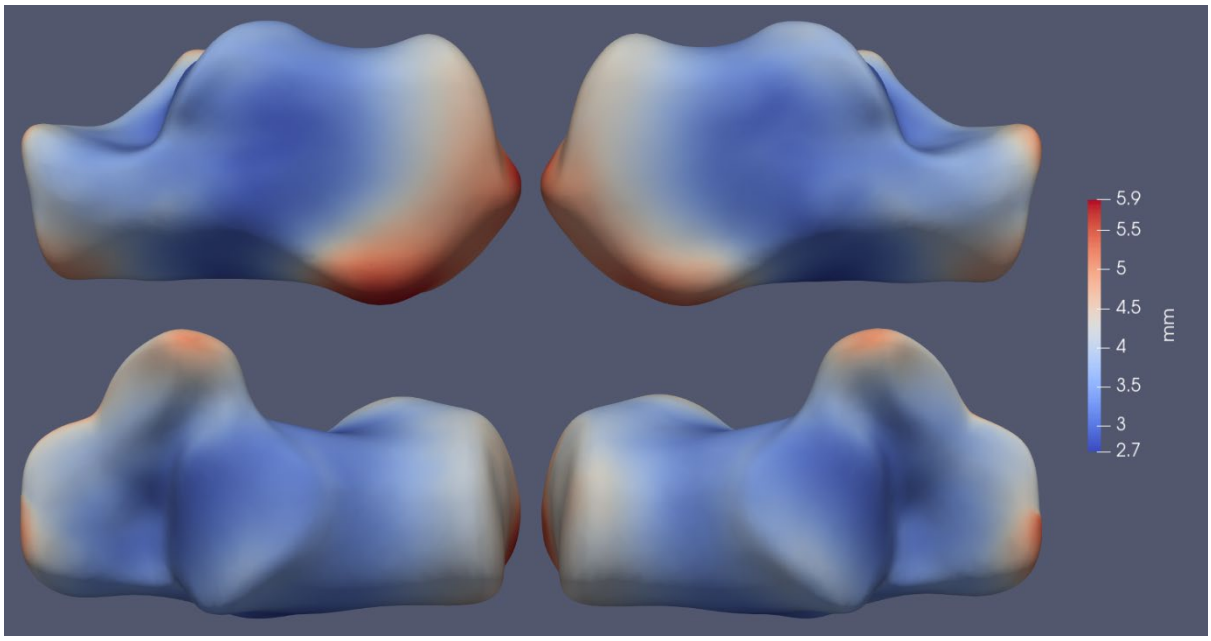

Figure 2. Lateral (top) and superior view (bottom) of the SSMs of the left and right calcaneus. The variances between the 41 subjects are represented by the colour coded distance map.

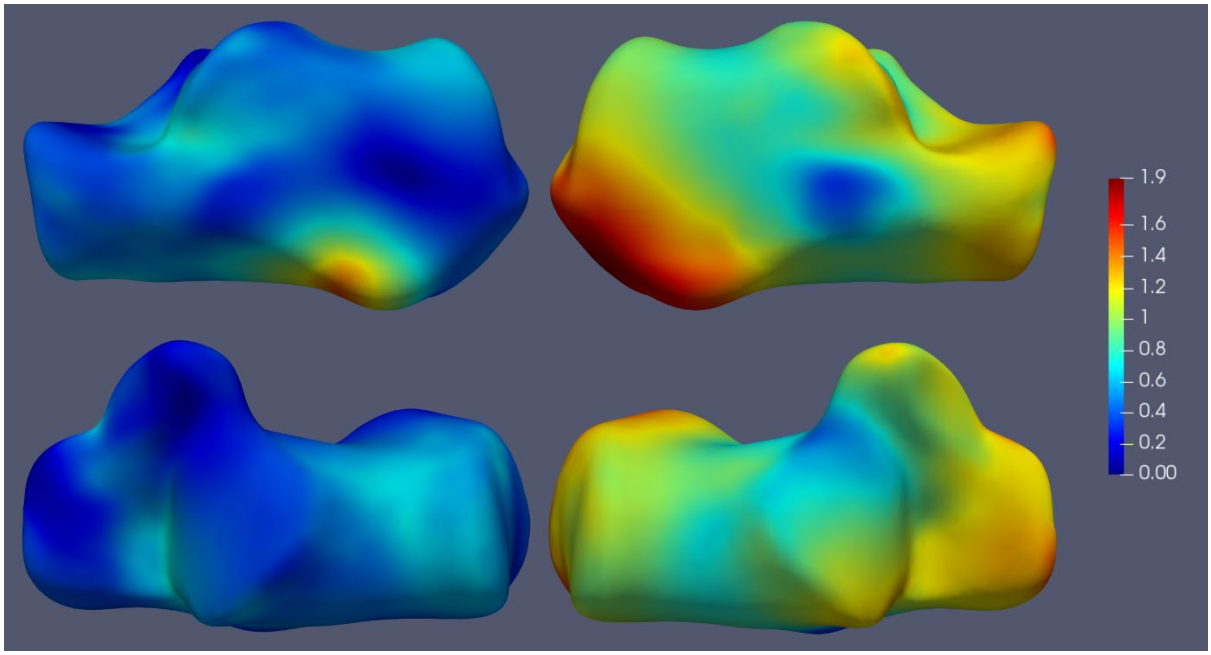

Figure 3. Colour coded linear regression map of the correlation between calcaneal anatomy and GAL-3D. Lateral and superior views of left and right mean SSM are shown, where a lager value indicates a stronger correlation with the angle measurement.

Table 1. Mean Gissane angles (degrees) of Japanese (n=10)

Gissane Angle	**Left**				**Right**				**L/R difference**
	Ave	SD	Min	Max	Ave	SD	Min	Max	P
GAL-3D	106.20	6.07	94.34	112.95	104.72	6.03	98.05	118.61	0.445
GAM-3D	89.74	6.69	80.87	104.22	89.06	5.98	81.82	102.75	0.721
GAC-3D	99.03	6.40	89.06	109.95	97.81	5.79	90.72	107.71	0.333
GAL-2D	107.77	7.37	92.94	120.65	104.40	6.31	97.50	119.49	0.508
GAM-2D	114.87	10.65	100.33	136.95	111.02	9.66	100.24	133.51	0.037
GAC-2D	106.50	7.15	94.04	116.86	104.78	6.30	97.90	114.92	0.285

Table 2. Mean Gissane angles (degrees) of Thai (n=31)

Gissane Angle	**Left**				**Right**				**L/R difference**
	Ave	SD	Min	Max	Ave	SD	Min	Max	P
GAL-3D	106.00	7.26	93.29	125.30	104.94	6.97	89.67	120.09	0.264
GAM-3D	88.99	5.83	77.74	103.68	89.17	6.10	76.85	103.22	0.784
GAC-3D	100.67	7.06	91.81	116.72	100.25	7.19	88.86	113.92	0.505
GAL-2D	106.54	8.98	90.43	129.71	104.83	6.99	89.76	119.42	0.299
GAM-2D	107.80	10.64	88.86	130.50	107.73	9.94	88.56	126.88	0.891
GAC-2D	107.12	8.33	96.00	123.78	106.57	8.64	92.65	123.48	0.518

Table 3. Difference and correlations between 3D and 2D Gissane angle measurements (n=41)

Gissane Angle	3D/2D Left angle difference		3D/2D Right angle difference		3D/2D Left angle correlation	3D/2D Right angle correlation
	deg	P	deg	P	Spearman's rho	Spearman's rho
GAL	0.14	0.033	0.16	0.051	0.990**	0.989**
GAM	20.35	0.000	19.38	0.000	0.839**	0.853**
GAC	6.69	0.000	6.48	0.000	0.941**	0.947**

**. Correlation is significant at the 0.01 level (2-tailed).

Table 4. Mean calcaneal maximal length (mm) from Asian subjects

Specimens	Left				Right				L/R difference
	Ave	SD	Min	Max	Ave	SD	Min	Max	P
All (n=41)	76.43	5.26	66.02	88.48	76.31	5.15	65.34	89.00	0.547
Japanese (n=10)	75.76	5.98	66.02	84.35	75.16	6.17	65.34	83.45	0.114
Thai (n=31)	76.64	5.09	67.95	88.48	76.68	4.83	67.04	89.00	0.845

Table 5. Correlations (Spearman's rho) between Gissane's angle and maximum calcaneal length

Gissane Angle	All		Japanese		Thai	
	Left	Right	Left	Right	Left	Right
GAL-3D	-0.089	0.314*	-0.297	0.455	0.029	0.237
GAM-3D	-0.182	0.096	-0.418	0.139	-0.063	0.065
GAC-3D	0.061	0.329*	-0.515	0.297	0.219	0.323
GAL-2D	-0.117	0.306	-0.418	0.467	0.013	0.225
GAM-2D	-0.084	0.136	-0.248	0.152	-0.019	0.150
GAC-2D	0.065	0.291	-0.212	0.248	0.176	0.289

*. Correlation is significant at the 0.05 level (2-tailed).

Table 6. Interclass correlation of five repeated GA measurements from two raters

Gissane Angle	LEFT: ICC of 5 Trials each				RIGHT: ICC of 5 Trials each			
	single	lower	upper	P	single	lower	upper	P
GAL-3D	0.932	0.579	0.977	0.000	0.895	0.757	0.950	0.000
GAM-3D	0.619	-0.450	0.889	0.000	0.633	-0.069	0.889	0.000
GAC-3D	0.925	0.270	0.979	0.000	0.929	0.506	0.977	0.000
GAL-2D	0.915	0.345	0.974	0.000	0.862	0.683	0.934	0.000
GAM-2D	0.950	0.865	0.978	0.000	0.879	0.778	0.935	0.000
GAC-2D	0.968	0.925	0.985	0.000	0.946	0.899	0.971	0.000

Table 7. Coefficients of linear regression between principal components and GAL-3D

	Left				Right			
	Estimate	Std. Error	t value	Pr(>|t|)	Estimate	Std. Error	t value	Pr(>|t|)
Intercept	106.279	0.343	310.079	0.000	104.936	0.345	303.880	0.000
PC 1	0.443	0.341	1.299	0.195	2.427	0.351	6.914	0.000
PC 2	-1.319	0.354	-3.723	0.000	-0.486	0.357	-1.359	0.175
PC 3	0.338	0.357	0.947	0.344	-0.054	0.348	-0.156	0.877
PC 4	-0.030	0.355	-0.084	0.933	-0.218	0.357	-0.611	0.541
PC 5	-0.028	0.344	-0.081	0.935	-0.495	0.353	-1.400	0.162
PC 6	-0.065	0.352	-0.184	0.854	0.647	0.355	1.820	0.070
PC 7	-3.576	0.351	-10.203	0.000	-0.846	0.362	-2.341	0.020
PC 8	0.271	0.362	0.748	0.455	1.297	0.348	3.727	0.000
PC 9	-1.015	0.357	-2.841	0.005	-1.318	0.358	-3.687	0.000
PC 10	-0.594	0.357	-1.663	0.097	-1.844	0.348	-5.300	0.000

Table 8. Normal range and mean values of Gissane's angle reported in previous studies compared to the values obtained in the present study

Study	Year	Reported min. and max.	Mean	No. of cases
Khoshhal et al. (Saudi Arabia)	2004	96-152	116.2±8.5	229
Seyahi et al. (Turkey)	2009	100-133	115.0±6.5	308
Shoukry et al. (Egypt)	2012	108-138	122.9±6.9	220
Sengodan et al. (India)	2012	100-145	126.8	204
Our study (Japanese)	2019	93-121	105.1±7.5	10
Our study (Thai)	2019	90-130	105.4±8.5	31